

Detection and Captioning with Unseen Object Classes

Berkan Demirel and Ramazan Gokberk Cinbis

Abstract—Image caption generation is one of the most challenging problems at the intersection of visual recognition and natural language modeling domains. In this work, we propose and study a practically important variant of this problem where test images may contain visual objects with no corresponding visual or textual training examples. For this problem, we propose a detection-driven approach based on a generalized zero-shot detection model and a template-based sentence generation model. In order to improve the detection component, we jointly define a class-to-class similarity based class representation and a practical score calibration mechanism. We also propose a novel evaluation metric that provides complimentary insights to the captioning outputs, by separately handling the visual and non-visual components of the captions. Our experiments show that the proposed zero-shot detection model obtains state-of-the-art performance on the MS-COCO dataset and the zero-shot captioning approach yields promising results.

Index Terms—zero-shot learning, zero-shot object detection, zero-shot image captioning



1 INTRODUCTION

The problem of generating a concise textual summary of a given image, known as *image captioning*, is one of the most challenging problems that require joint vision and lingual modeling. With ever increasing recognition rates in deep object detection models, pioneered by works such as [1], [2], [3], [4], [5], [6], [7], [8], [9], [10], [11], there have been a recent interest in generating visually grounded image captions via constructing detection-driven captioning models, *e.g.* [12], [13], [14], [15]. However, the success of such approaches are inherently limited by the set of classes spanned by the training set for the detector, which is typically too small to construct a visually comprehensive model. Therefore, such models are prone to synthesizing irrelevant captions in realistic, uncontrolled settings where input images may contain instances of completely novel object classes.

In the context of image classification, *zero-shot learning* (ZSL) has emerged as a promising alternative towards overcoming the practical limits in collecting labeled image datasets and constructing image classifiers with very large object vocabularies. ZSL approaches typically tackle the problem of transferring visual and/or semantic knowledge from the *seen* classes (training classes) to *unseen* classes (test-only classes). For the transfer, a variety of semantic knowledge sources are utilized, such as attributes [16], [17], class hierarchies [18], [19], attribute-to-class name mappings [20], label relation graphs [21]. While accurate ZSL is still an open problem, significant progress has been made in recent years in zero-shot image classification [22]. Very recently, a few

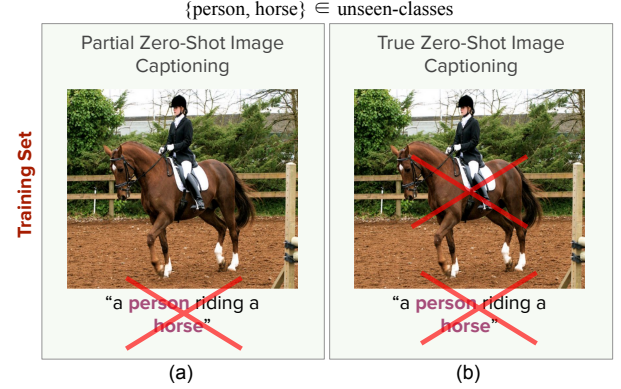


Fig. 1: (a) *Partial zero-shot image captioning* problem, where the visual examples, without captions, of *unseen* classes are used during training. (b) *True zero-shot image captioning* problem, neither visual nor textual examples of *unseen* classes are available during training.

methods have also been proposed for the *zero-shot object detection* (ZSD) problem [23], [24], [25], [26], [27].

In a similar manner, *zero-shot image captioning* (ZSC), where the task is to create captions of images containing object classes unseen at the training time, aims to develop methods towards overcoming the data collection bottleneck in image captioning. However, we observe that there is no benchmark or prior work, except the preliminary conference version of this paper, directly tailored to study captioning in a *true* zero-shot setting: while there are few recent works on ZSC [15], [28], these methods study the *zero-shot* problem only in the language domain, presuming the availability of a pre-trained fully-supervised object detector over all object classes of interest, to the best of our knowledge. We name these methods *partial zero-shot image captioning* methods because of the availability of a pre-trained fully-supervised object detectors covering all classes of interest.

- B. Demirel is with the Department of Computer Engineering, Middle East Technical University, Ankara, Turkey and also with the HAVELSAN Inc. E-mail: berkan.demirel@metu.edu.tr
- R. G. Cinbis is with the Department of Computer Engineering, Middle East Technical University, Ankara, Turkey. E-mail: gcinbis@ceng.metu.edu.tr

This work was supported in part by the TUBITAK Grant 116E445 and 119E597.

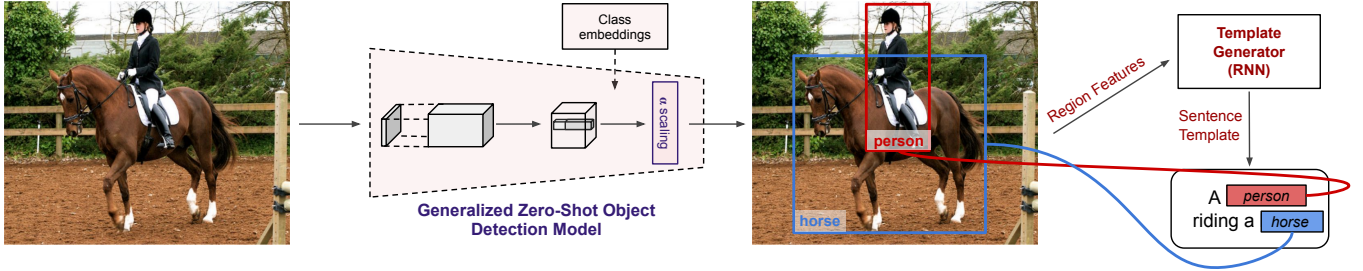


Fig. 2: Our zero-shot captioning framework, which consists of two components: (i) a generalized zero-shot object detection model with scaling based score calibration, and (ii) an image caption generation module.

Following these observations, we propose the problem of *true zero-shot captioning*, where test images contain instances of object categories with no supervised visual or textual examples, in addition to the categories with training instances. We believe that this change constitutes a more direct problem definition towards (i) developing semantically scalable captioning methods, and, (ii) evaluating captioning approaches in a realistic setting where not all object classes have training examples. The difference between the partial versus true zero-shot image captioning problems is illustrated in Figure 1.

To tackle the true zero-shot captioning problem, we propose a ZSC approach that consists of a novel GZSD model and a template-based [15] caption generator defined over the GZSD outputs. A high-level summary of our ZSC approach can be found in Figure 2. The ZSC problem naturally requires a generalized zero-shot detection (GZSD) model, since test scenes may contain both seen and unseen class instances. In order to address the GZSD problem, we propose a scaling scheme and incorporate *uncertainty calibration* [29] to make seen and unseen class scores comparable. We also find out that using class-to-class similarities obtained over word embeddings [30] between each target class and all training classes as *class embeddings* improves GZSD results, compared to using original class name embeddings. On the MS-COCO dataset [31], we present a detailed evaluation of both ZSC and GZSD models. For a more accurate evaluation of the ZSC results, we propose a new evaluation metric called V(visual)-METEOR, which adapts and improves the widely used METEOR metric for zero-shot captioning evaluation purposes.

In summary, this work aims to make conceptual, technical and experimental contributions on image captioning. First, we define a new paradigm for image captioning problem where some of the test classes are unseen both visually and textually. Second, we propose and thoroughly evaluate a novel GZSD approach, which yields state-of-the-art zero-shot object detection results and plays a central role in the construction of our ZSC model. Third, we point out and study new challenges regarding the evaluation of captioning systems in true zero-shot settings.

A preliminary version of this work has previously appeared in [32]. In addition to providing a more detailed discussion of the related work and presentation of the approach, this paper extends the previous version in the following major ways: we extend the GZSD study by in-

roducing the uncertainty calibration loss and providing a more thorough evaluation of the approach. We specifically evaluate the impact of important model decisions, introduce a comparison to the state-of-the-art on the benchmark MS-COCO dataset, and analyze the failure patterns of the GZSD model. We quantitatively demonstrate the advantage of using class-to-class similarities, instead of directly using word embeddings, as class embeddings. We similarly extend the evaluation of the zero-shot captioning model, most significantly by extending discussion on the challenges in zero-shot captioning and proposing the new V-METEOR metric.

The rest of the paper is organized as follows: Section 2 presents an overview of closely related works. Section 3 describes the proposed GZSD method. Section 4 describes the way we construct the zero-shot captioning approach on top of the GZSD model and defines the proposed V-METEOR metric. Section 5 presents the experimental evaluation of the GZSD and ZSC models. Section 6 presents the concluding remarks.

2 RELATED WORK

Below, we provide an overview of the related work on zero-shot learning for image classification, zero-shot object detection and image captioning.

2.1 Zero-shot learning

Early work on ZSL focused on directly using attribute based probabilistic models for transferring semantic information from seen to unseen classes [33]. More recent works explore other mediums and discriminative models for knowledge transfer. Akata *et al.* [16] proposes to a discriminatively learned compatibility model over image features and attribute based class embeddings. Akata *et al.* [19] suggests the use of class hierarchies and distributed word representations of class names as alternatives to handcrafted attributes. Demirel *et al.* [20] utilizes attribute name embeddings to construct higher-level image representations for class name based zero-shot learning. Other notable approaches include synthesized classifiers [34], semantic autoencoders [35], hierarchy graphs [21], diffusion regularization [36], attribute regression [37] and latent space encoding [38]. A comparative survey of zero-shot learning models can be found in Xian *et al.* [22], which also introduces the problem of *generalized zero-shot learning* (GZSL) problem in an image classification context.

One of the main challenges in GZSL is the ability to produce models that can yield comparable scores for seen and unseen classes. In particular, discriminatively learned classification models, trained over seen class samples, tend to yield higher confidence scores for seen classes even on the test samples of unseen classes. A line of work aims to address this problem through techniques specifically for reducing the prediction bias towards the seen classes. For this purpose, Liu *et al.* [39] proposes to increase unseen class prediction confidence by minimizing the entropy of unseen class scores during training. Jian *et al.* [40] estimates unseen to seen class similarities based on the sparse coding of class embeddings, and promotes higher confidence scores for related unseen classes during training. Song *et al.* [41] proposes a transductive learning framework to reduce the seen class bias. Chao *et al.* [42] uses an empirically chosen calibration coefficient for scaling the seen class scores. We utilize a similar strategy for GZSD, except that instead of manually choosing the scaling coefficient, we learn it during training.

Alternatively, sample synthesizing generative models have recently been proposed for (G)ZSL. These methods aim to build class embedding conditional models that can be used to generate synthetic training samples for unseen classes. Data generating GZSL approaches are attractive for naturally addressing the seen class bias problem, at the cost of typically being computationally more demanding and formulationally more complex than purely discriminative approaches. Being one of the first works in this direction, Bucher *et al.* [43] proposes to build feature-space generative models. Felix *et al.* [44] proposes to use data reconstruction for model regularization, based on multi-modal cycle consistency loss term. Mishra *et al.* [45] propose a conditional Variational Autoencoder (VAE) [46], [47] based model. Xian *et al.* [48] improves conditional VAEs via adversarial training. Zhu *et al.* [49] proposes to learn textual description conditional generative models. Li *et al.* [50] utilizes conditional Wasserstein GANs [50]. Sariyildiz and Cinbis [51] propose gradient matching loss to improve the quality of the generated samples. Elhoseiny and Elfeki [52] studies incorporation of losses that directly aim to increase sample variations.

2.2 Zero-shot object detection

The most recent object detection methods can be categorized into the following two groups: (i) regression-based approaches, and, (ii) region proposal-based approaches. Regression-based approaches generate all candidate detection scores and positions jointly in a single step, using a single convolutional network [1], [2], [8], [11], [53], [54]. Region proposal-based approaches instead first generate region proposals, then classify (and update) each region proposal [3], [4], [6], [7], [10], [55], [56]. Recently, zero-shot object detection methods have been proposed [23], [24], [25], [26], [27], [57], [58], typically as extensions of supervised object detection models. Among these studies, Bansal *et al.* [25] proposes a two-step approach which first locates object proposals from low-level features [59] and then classifies the resulting candidate regions using a ZSL model. Rahman *et al.* [24] proposes a region proposal-based approach and uses

a semantic clustering based loss term to bring similar classes closer to each other. Demirel *et al.* [23] proposes a regression-based ZSD model that jointly incorporates two ZSL models based on convex combinations of semantic embeddings [60] and bi-linear compatibility models [16]. Rahman *et al.* [26] proposes a polarity loss term that is based on the focal loss approach, to tackle better alignment between visual and semantic domains. Hence, semantic representations of visually similar classes get closer to each other. Li *et al.* [57] uses natural language descriptions of classes for ZSD. Shao *et al.* [58] focuses on candidate proposal generation problem of unseen classes in the ZSD and show the impact of the candidate object proposal generation ability of the object detectors for unseen classes.

The ZSD approach closest to the model that we build for ZSC in this work is the one proposed by Demirel *et al.* [23]. Our approach differs by (i) leveraging class-to-class similarities measured in the word embedding space as class embeddings, as opposed to directly using the word embeddings, (ii) learning a class score scaling coefficient that reduces the seen class bias and improves generalized zero-shot detection accuracy, and (iii) exploring the use of uncertainty calibration [29] in GZSD.

There exists alternative learning paradigms that also aim to reduce the dependency on fully-supervised training examples for object detection. To this end, methods for transforming image classifiers into object detectors, *e.g.* [1], [61], [62], and image-level label based weakly supervised learning approaches, *e.g.* [63], [64], [65], stand out as closely related directions. However, such approaches still require labeled training images for all classes of interest, which can be a major obstacle in building models with semantic richness needed for captioning.

2.3 Image captioning

Most recent image captioning approaches are based on deep neural networks [12], [15], [66], [67], [68], [69], [70]. Mainstream methods can be categorized as (i) template-based techniques [12], [15], [71] and (ii) retrieval-based ones [69], [72], [73], [74]. Template-based captioning approaches generate templates with empty slots, and fill those slots using attributes or detected objects. Kulkarni *et al.* [12] builds conditional random field (CRF) models to push tight connections between the image content and sentence generation process before filling the empty slots. Farhadi *et al.* [71] uses triplets of scene elements for filling the empty slots in generated templates. Lu *et al.* [15] uses a recurrent neural network to generate sentence templates for slot filling. Retrieval-based image captioning methods, in contrast, rely on retrieving captions from the set of training examples. More specifically, a set of training images similar to the test example are retrieved and the captioning is performed over their captions.

In this work, we aim to generate captions that can include classes that are not seen in the supervised training set, where retrieval-based approaches are not directly suitable. For this reason, we adopt a template-based approach that generates sentence templates and fills the visual word slots with the GZSD model predictions.

Dense captioning [75], [76], [77] appear to be similar to the zero-shot image captioning, but the focus is significantly

different: while dense captioning aims to generate rich descriptions, our goal in ZSC is to achieve captioning over novel object classes. Some captioning methods go beyond training with fully supervised captioning data and allow learning with a captioning dataset that covers only some of the object classes plus additional supervised examples for training object detectors and/or classifiers for all classes of interest [13], [28], [78], [79], [80]. Since these methods presume that all necessary visual information can be obtained from some pre-trained object recognition model, we believe they cannot be seen as true zero-shot captioning approaches.

In our work, we additionally look into the problem of evaluating image captioning results with a focus on zero-shot image captioning. The evaluation of image captioning methods is not a *solved* problem. There are well-known metrics, such as METEOR [81] and SPICE [82], which are widely used in image captioning. There are also recent works to improve existing captioning metrics, such as the work of Wang *et al.* [83], which aims to improve SPICE by incorporating uniqueness and descriptiveness aspects into the metric. In this paper, we aim to build a metric that allows per-class joint evaluation of visual and lingual caption quality so that we can explicitly evaluate unseen (and seen) class captioning quality. For this purpose, we define a new visual class-sensitive metric by extending the n-gram based METEOR metric.

3 ZERO-SHOT OBJECT DETECTION

Our zero-shot captioning approach composes of a generalized zero-shot object detector and a detection-driven image caption generator. In this section, we explain the details of our GZSD model. We then describe how we build the final ZSC model in the following section.

3.1 Main zero-shot detection model

In zero-shot object detection, the goal is to learn a detection model over the examples given for the seen classes such that the detector can recognize and localize the bounding boxes of the instances of all classes $Y = Y_s \cup Y_u$, where Y_s and Y_u represents the set of seen and unseen classes, respectively. For this purpose, we use the YOLO [2] architecture as our backend, and adapt it to the GZSD problem.

In the original YOLO approach, the loss function consists of three components: (i) the localization loss, which measures the error between ground truth locations and predicted bounding boxes, (ii) the objectness loss, and, (iii) the recognition loss. The original recognition loss ℓ_{cls} is defined in terms of a squared error function over class posterior probabilities at each cell, in a grid of size $S \times S$ ($S = 13$, by default):

$$\ell_{cls}(x) = \sum_{i=0}^{S^2} \mathbb{1}_{obj}^i \sum_{c \in Y_s} (t(x, c, i) - f(x, c, i))^2 \quad (1)$$

where the target indicator mapping $t(x, c, i)$ is 1 if the cell i of image x contains an instance of class c and otherwise 0. $f(x, c, i)$ is the prediction score corresponding two the class c and cell i . $\mathbb{1}_{obj}^i = 1$ if an object instance appears in cell i , and 0 otherwise.

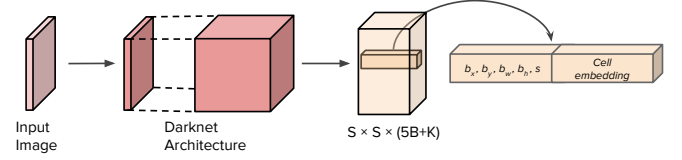


Fig. 3: Summary of the proposed zero-shot detection method. At each cell, the network is trained to produce box coordinate predictions (denoted by b_x, b_y, b_w, b_h in the figure), objectness scores (denoted by s in the figure) and a cell embedding to be used for zero-shot recognition.

Following our prior work in [23], we adapt the YOLO model to the GZSD problem by replacing per-cell class probability predictions with *cell embeddings* and re-defining the prediction function as a compatibility estimator between the cell embeddings and class embeddings:

$$f(x, c, i) = \frac{\Omega(x, i)^T \Psi(c)}{\|\Omega(x, i)\| \|\Psi(c)\|} \quad (2)$$

Here, $\Omega(x, i)$ denotes the predicted cell embedding, in addition to the box predictions obtained for the image cell i for the input image x , as shown in Figure 3. $\Psi(c)$ represents the c -th class embedding. The resulting model, therefore, allows making detection predictions for samples of novel classes purely based on their class embeddings.

Class embeddings. In principle, one can use attributes or word embeddings of class names directly as class embeddings, as done in [23]. Attributes can provide powerful visual descriptions of classes, however, they tend to be domain specific and typically difficult to define for a large variety of object classes, as needed in zero-shot captioning. Word embeddings of class names, which are obtained from language models self-supervisedly trained on unlabeled text corpora (e.g. Word2Vec [30], GloVe [84]), are much easier to collect. However, word embeddings typically contain indirect information about the visual characteristics of classes, and, therefore, known to provide significantly weaker prior knowledge for visual recognition [19].

To use class name word embeddings more effectively, we propose to use class-to-class similarities, computed over word embeddings, instead. More specifically, we define the class embedding for the class c as the vector of similarities between c and each reference training class \bar{c} :

$$\Psi(c) = \left[\varphi(c)^T \varphi(\bar{c}) + 1 \right]_{\bar{c} \in Y_s} \quad (3)$$

where $\varphi(c)$ denotes the c -th class name’s word embedding. Since semantic relations across classes tend to correlate with their visual characteristics, this embedding can provide a valuable implicit visual description defined through a series of inter-class similarities. The ZSL method, therefore, can make predictions based collectively on these similarity values. We empirically demonstrate the advantage of the similarity-driven embeddings in Section 5.

3.2 Generalized zero-shot detection extensions

We need to obtain a generalized zero-shot detector, where both training and test classes may appear at the test images.

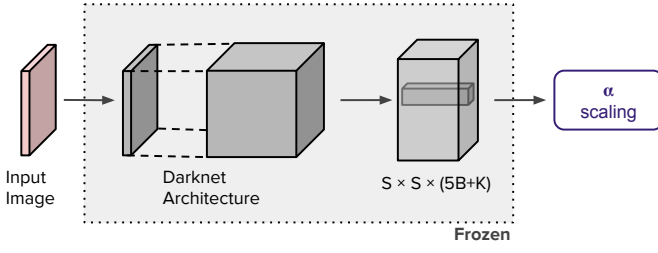


Fig. 4: α scaling factor learning process. In the short second round of the learning, all layers of the YOLO-based ZSD method are frozen. The α value is learned through the training set in a few epochs.

However, there can still be a significant bias towards the seen classes, as the detection model is trained to maximize one of the seen class probabilities on each positive training example. The following paragraphs explain two extensions that we explore to improve generalized zero-shot detection performance: (i) *alpha scaling*, and (ii) *uncertainty calibration*.

Alpha scaling. We aim to overcome the seen class bias problem by a scaling factor that aims to make unseen class scores more comparable to those of the seen classes. This additional scaling factor focuses on removing bias towards training classes using the existing training set without requiring additional examples. For this purpose, we introduce the α coefficient for the unseen test classes by redefining $f(x, c, i)$ as follows:

$$f(x, c, i) = \begin{cases} \alpha \frac{\Omega(x, i)^T \Psi(c)}{\|\Omega(x, i)\| \|\Psi(c)\|}, & \text{if } c \in Y_u \\ \frac{\Omega(x, i)^T \Psi(c)}{\|\Omega(x, i)\| \|\Psi(c)\|}, & \text{otherwise} \end{cases} \quad (4)$$

In order to optimize the coefficient α , we first train the ZSD model over all training classes without α . We then designate a subset of seen classes as *unseen-imitation* classes. To approximately obtain unseen like confidence scores for these classes, we temporarily set all entries corresponding to unseen-imitation classes in Eq. 3 to zeros and treat unseen-imitation classes as unseen classes in Eq. 4. These modifications allows us to obtain classification scores as if the model was trained without using samples of unseen-imitation classes. We then train only the α coefficient, keeping the rest of the network frozen, as shown in Figure 4.

Overall, the proposed α coefficient learning scheme leverages the special structure of our class embeddings to efficiently approximate the unseen class scores. While the approximation can possibly be coarse, we experimentally show in Section 5 that the proposed scheme is effective for learning the α coefficient, at a negligible extra training cost.

Uncertainty calibration. The second technique that we explore to improve generalized zero-shot detection performance is *uncertainty calibration*, which we adapt from the zero-shot image classification approach of Liu *et al.* [29]. The main idea here is to minimize the uncertainty over unseen class predictions during model training. This approach is rooted in the observation that a prediction model learned

over seen class samples tend to yield lower confidence scores for unseen classes, resulting in misdetections.

The uncertainty in confidence scores is quantified via entropy over unseen class probabilities. We adapt the uncertainty calibration loss ℓ_h to our zero-shot detector as a loss over per-cell predictions, as follows:

$$\ell_h(x) = - \sum_{i=0}^{S^2} \mathbb{1}_{obj}^i \sum_{c \in Y_u} p_u(c|x, i) \log p_u(c|x, i) \quad (5)$$

Here, $p_u(\cdot)$ corresponds to $f(x, c, i)$ -driven unseen class likelihoods:

$$p_u(c|x, i) = \frac{\exp(f(x, c, i)/\tau)}{\sum_{c' \in Y_u} \exp(f(x, c', i)/\tau)} \quad (6)$$

where τ denotes the softmax temperature coefficient. τ is empirically determined as suggested for zero-shot classification in Liu *et al.* [29]. The loss encourages more confident unseen class score estimates, as less ambiguous predictions results in smaller entropy values. In order to adapt the uncertainty calibration to the detection model, we first train the ZSD model over all training classes as in the alpha scaling optimization process. We also use the same designated unseen-imitation subset as unseen classes. In the second training stage, we temporarily set all entries corresponding to unseen-imitation classes to zeros and then fine-tune the whole model without freezing any layers, unlike alpha scaling coefficient learning.

3.3 Final training objective

The final loss function, including the main ZSD training loss terms and GZSD extensions, takes the following form::

$$\begin{aligned} L = & \sum_{i=0}^{S^2} \mathbb{1}_{obj}^i [(b_{x_i} - \hat{b}_{\hat{x}_i})^2 + (b_{y_i} - \hat{b}_{\hat{y}_i})^2] \\ & + \sum_{i=0}^{S^2} \mathbb{1}_{obj}^i [(\sqrt{b_{w_i}} - \sqrt{\hat{b}_{\hat{w}_i}})^2 + (\sqrt{b_{h_i}} - \sqrt{\hat{b}_{\hat{h}_i}})^2] \\ & + \sum_{i=0}^{S^2} \mathbb{1}_{obj}^i (s_i - \hat{s}_i)^2 + \sum_{i=0}^{S^2} \mathbb{1}_{noobj}^i (s_i - \hat{s}_i)^2 \\ & + \sum_{i=0}^{S^2} \mathbb{1}_{obj}^i \sum_{c \in Y_s} [t(x, c, i) - f(x, c, i)]^2 \\ & - \sum_{i=0}^{S^2} \mathbb{1}_{obj}^i \sum_{c \in Y_u} p_u(c|x, i) \log(p_u(c|x, i)) \end{aligned}$$

where b_x, b_y, b_w and b_h denote bounding box coordinates. The s term represents the objectness score. Symbols with a hat are ground-truth values and others represent the corresponding predictions. For simplicity, here we express the formula as if a single prediction per cell is being made, however, the model generates multiple predictions per cell in practice. The sequence of loss terms correspond to enforcement of the following goals: (i) correct localization of cell centers, (ii) correct width and height predictions for bounding boxes, (iii) estimation of objectness scores equal to the IoU in each cell with an associated target ground-truth box, (iv) estimation of objectness scores as zero in case

of no target object, (v) maximize the compatibility between cell embeddings and class embeddings, and (vi) uncertainty calibration for unseen classes, respectively. We note that the uncertainty calibration loss is used only in the second stage of detector training.

4 ZERO-SHOT IMAGE CAPTIONING

In this section, we first explain how we build the zero-shot captioning model on top of our GZSD model, and then we discuss the evaluation difficulties and define our V-METEOR zero-shot captioning quality metric.

4.1 Zero-shot captioning model

Our goal is the construction of an image captioning model that can accurately summarize scenes potentially with seen and unseen class instances. For this purpose, we opt to use a template-based captioning method which provides the sentence templates with visual word slots are to be filled based on the outputs of an object recognition model. While prior works use supervised detection models for object recognition (Section 2), here we incorporate our GZSD model.

As the template-based captioning approach, we use the slotted sentence template generation model of Neural Baby Talk (NBT) [15] in our work. The NBT method generates sentence templates which consist of the empty word slots by using a recurrent neural network. To obtain a content-based attention mechanism over the grounding regions, NBT embraces the *pointer networks* approach [85]. Hence, the purpose of the NBT is to yield a visually grounded caption q on a given image x and a set of image regions obtained from GZSD model. In this context, NBT model updates model parameters ω to maximize the log likelihood of the ground-truth captions over the image and text training pairs (x, q) :

$$\omega^* = \arg \max_{\omega} \sum_{(x, q)} \log p(q|x; \omega). \quad (7)$$

Here, the conditional caption likelihood $p(q|x; \omega)$ of $|q|$ words is measured auto-regressively, using a recurrent network:

$$p(q|x; \omega) = \prod_{t=1}^{|q|} p(q_t|q_{1:t-1}, x; \omega). \quad (8)$$

The NBT method additionally incorporates a latent variable r_t to represent the specific image region, so the probability of a word q_t is modeled as follows:

$$p(q_t|q_{1:t-1}, x; \omega) = p(q_t|r_t, q_{1:t-1}, x; \omega)p(r_t|q_{1:t-1}, x; \omega). \quad (9)$$

Here, the NBT defines two word types for q_t , corresponding to *textual* and *visual* words. Textual words are not directly related to any image region or specific visual object instance, therefore the model provides only dummy grounding for them. The template generation network uses the object detection outputs to fill empty visual word slots, where we utilize the outputs of our GZSD model.

We train both the zero-shot detection model and the sentence template generation component of NBT over examples containing only the seen class instance annotations,

as required by the *true zero-shot image captioning* protocol. At test time, we use the GZSD outputs over all classes as inputs to the NBT sentence generator.

4.2 Measuring zero-shot captioning quality

Partial zero-shot image captioning approaches use existing captioning metrics, such as METEOR [81], SPICE [82] and F1 score, for evaluation purposes. While these generic textual similarity based metrics provide useful information about the quality of captioning results, they do not explicitly handle the problem of capturing visual content within the generated sentence. Therefore, such metrics can possibly be heavily influenced by structural and syntactical similarities across generated and ground-truth sentences. Exceptionally, F1 score differs in this regard by completely ignoring the sentence structure and measuring only the coverage of (unseen) class names within captions. However, F1 score fails to measure the overall quality or accuracy of the generated sentences, which is also clearly important.

We observe that, based on our experiments in Section 5, the explicit handling of visual and non-visual content in the evaluation of sentences is particularly necessary for *true zero-shot image captioning*. In this setting, the problem of generating sentences that summarize the visual content accurately, including visual entities that are completely unseen during training, is fundamentally challenging, especially in comparison to partial zero-shot captioning with fully-supervised visual recognition models. Therefore, in this section, we propose a new captioning evaluation metric as a step towards formalizing better metrics for true zero-shot captioning.

We develop our metric based on METEOR, which is known to be a simple yet effective metric that yields strong correlation with human judgment [86]. The original METEOR metric is defined by the following formula:

$$\text{METEOR} = F_{\text{mean}}(1 - p) \quad (10)$$

where F_{mean} aims to capture correctness in terms of unigram precision and recall values and p is a penalty term for evaluating the overall sentence compatibility. More specifically, F_{mean} is given by:

$$F_{\text{mean}} = \frac{10PR}{R + 9P} \quad (11)$$

where P and R are the unigram precision and unigram recall values, respectively. These are calculated as:

$$P = \frac{m}{w_t} \quad (12)$$

$$R = \frac{m}{w_r} \quad (13)$$

where m is the number of unigrams in both reference and generated captions, w_t is the number of unigrams in the candidate caption and w_r is the number of unigrams in the reference caption. The p penalty term checks how well textual chunks match between a pair of reference and generated captions, using the following definition:

$$p = 0.5 \left(\frac{c}{u_m} \right)^3 \quad (14)$$

where c is number of maximally long matching subsequences, and u_m is number of mapped unigrams.

We extend the METEOR metric by defining two separate F_{mean} metrics for the visual and non-visual entities. For this purpose, we compute F_{mean}^v and F_{mean}^n , similar to Eq. 11, separately over only visual words and only non-visual words, respectively. We, then, define the proposed metric V-METEOR based on their harmonic mean, as follows:

$$\text{V-METEOR} = \frac{2F_{\text{mean}}^v F_{\text{mean}}^n}{F_{\text{mean}}^v + F_{\text{mean}}^n} (1 - p) \quad (15)$$

In this manner, the proposed V-METEOR metric explicitly measures the joint visual or non-visual accuracy of a sentence, through the harmonic mean of the F_{mean}^v and F_{mean}^n terms. It also incorporates the overall sentence similarity by keeping the penalty term (p) as in METEOR.

To be able to measure per-class captioning quality, which is particularly valuable in the zero-shot captioning context, we separately compute V-METEOR for each class. In calculation of the V-METEOR score of a sentence for a class, the words corresponding to the class name are considered as the visual words, and the words that are not corresponding to any one of the class names are considered as non-visual words. The overall V-METEOR score is obtained by averaging per-class scores.

Finally, we additionally define the following two variations of the V-METEOR metric, for separately measuring the visual and non-visual quality of the generated sentences, respectively:

$$\text{V-METEOR}_{\text{vis}} = F_{\text{mean}}^v (1 - p) \quad (16)$$

$$\text{V-METEOR}_{\text{nvis}} = F_{\text{mean}}^n (1 - p) \quad (17)$$

We use all three versions of the V-METEOR metric in our experiments to make a relatively more complete assessment of the results.

5 EXPERIMENTS

In this section, we present detailed analysis of our GZSD and ZSC approaches. We first explain the experimental setup, including datasets, splits and word embedding details, in Section 5.1. We then report the implementation details and discuss the experimental results for the GZSD model, ZSC model and V-METEOR metric in Section 5.2, Section 5.3 and Section 5.4, respectively. Finally, we present additional complementary analyses in Section 5.5.

5.1 Experimental setup

Zero-shot detection and (partial) zero-shot captioning works use different splits of the MS-COCO dataset for historical reasons. To make our results comparable to related works, we use the same splits as in the related works, separately for the GZSD and ZSC experiments, as explained below.

GZSD evaluation. We use MS-COCO [31] dataset in our experiments. We compare our GZSD method with SB [25], DSES [25], FL-65 [26], HRE [23], FL-80 [26] and TL [27] approaches. We use the same dataset splits and settings with them in our main GZSD experiments to make fair comparisons. We follow the dataset settings described in [26], which incorporates all 80 MS-COCO classes. According

Method	seen/unseen	seen	unseen	HM
SB [25]	48/17	-	0.70	-
DSES [25]	48/17	-	0.54	-
FL-65 [26]	65/15	37.56	10.80	16.77
FL-80 [26]	65/15	40.60	10.28	16.40
HRE [23]	65/15	28.40	12.80	17.65
TL [27]	65/15	28.79	14.05	18.89
SimEmb-base (w/o α)	65/15	28.54	12.45	17.34
SimEmb	65/15	28.91	15.78	20.41
SimEmb*	65/15	28.87	16.00	20.59

TABLE 1: mAP results on MS-COCO dataset with GZSD (65/15) settings. The last three rows correspond to the following versions of our method: **SimEmb-base** represents the model without α scaling for unseen classes, **SimEmb** represents the model with the trained α scaling and **SimEmb*** represents the model with empirically the best alpha scaling coefficient with respect to the harmonic mean (HM) metric.

to this dataset split, 65 classes are used as the training classes and the remaining 15 (*i.e. airplane, train, parking meter, cat, bear, suitcase, frisbee, snowboard, fork, sandwich, hot dog, toilet, mouse, toaster and hair drier*) as the test classes.

ZSC evaluation. For the ZSC approach, we compare the proposed approach with selected *upper-bound* methods from [13], [15], [28], [78], [79]. We again use the same dataset splits and settings as in these works. In this problem, 8 of 80 MS-COCO classes are used as unseen classes, namely: *bottle, bus, couch, microwave, pizza, tennis racket, suitcase and zebra*. During training, we use the MS-COCO training set that do not contain any objects or textual representations belonging to a class from the seen class list. For evaluation, we use the evaluation split defined in Hendricks *et al.* [13].

Word embeddings. As part of the GZSD model, we use 300-dimensional word2vec [87] embeddings of class names. For the class names containing more than one word, *e.g. tennis racket*, we take the average of the per-word embeddings. We use 300-dimensional GloVe vector embeddings [84] in the template generation component of the ZSC, following the NBT approach [15].

5.2 Zero-shot object detection

In this section, we report and discuss experimental results for the GZSD model. We build our GZSD model based on the YOLO [2] approach. We train the model for 160 epochs with a learning rate of 0.001, and a batch size of 32. This training is conducted on the MS-COCO dataset using training set of 65 seen classes. Once the main zero-shot detection model is trained, we select 8 out of 65 seen classes as *unseen-imitation* classes for alpha scaling optimization and uncertainty calibration purposes, as explained in Section 3.2. For the alpha scaling and uncertainty calibration training stages, we continue training for 10 more epochs. We use mean average precision (mAP) metric to compare GZSD methods.

Main results. We present the experimental results in Table 1. The upper part of the table presents results of the state-of-the-art techniques, including SB [25], DSES [25], FL-65 [26], FL-80 [26], HRE [23] and TL [27]. The lower part of the

Figure 1 is a line graph showing Accuracy (Y-axis, ranging from 10 to 35) versus Alpha (X-axis, ranging from 1.0 to 2.0). The graph compares the performance of three models: HM (blue line with circles), Seen (orange line with crosses), and Unseen (green line with squares). The HM model shows the highest accuracy, peaking around 20.5% at Alpha = 1.4. The Seen model shows the lowest accuracy, peaking around 28.5% at Alpha = 1.4. The Unseen model shows the lowest accuracy, peaking around 15.5% at Alpha = 1.4. The legend indicates: HM (blue line with circles), Seen (orange line with crosses), and Unseen (green line with squares).

Alpha	HM Accuracy	Seen Accuracy	Unseen Accuracy
1.0	17.2	28.5	12.5
1.1	18.5	28.5	13.8
1.2	20.0	28.5	15.5
1.3	20.5	28.8	15.8
1.4	20.5	28.5	15.8
1.5	20.5	28.2	15.8
1.6	20.2	28.0	15.8
1.7	19.8	27.2	15.5
1.8	19.2	26.2	15.2
1.9	18.2	25.2	14.5
2.0	17.8	24.2	14.2

table presents the results based on our approach, which we call *SimEmb*. The first row in the lower part of the table, *i.e.* **SimEmb-base**, represents the main model excluding the α scaling coefficient for unseen classes. SimEmb-base method obtains 28.54% mAP on seen classes, 12.45% mAP on unseen classes and 17.34 harmonic mean (HM) value. The second row, *i.e.* **SimEmb**, represents the version that incorporate the learned α scaling coefficient (without uncertainty calibration). SimEmb obtains 28.91% mAP on seen classes, 15.78% mAP on unseen classes and 20.41% harmonic mean value. Finally, **SimEmb*** represents an upper-bound reference model, where alpha scaling coefficient is empirically tuned on the test set to maximize the HM score by evaluating for a range of α values. This upper-bound model obtains 28.87% mAP on seen classes, 16.00% mAP on unseen classes and 20.59 HM value.

α -scaling	uc-calib	seen	unseen	HM
		28.54	12.45	17.34
	✓	28.60	11.15	16.04
✓		28.91	15.78	20.41
✓	✓	28.85	15.85	20.46

SimEmb-base, show that alpha scaling coefficient is crucial for obtaining higher accuracy on unseen classes detections and alpha scaling do not disrupt the seen class performance. Finally, the comparison between SimEmb and the upper-bound SimEmb* models show that the proposed alpha scaling learning scheme is effective as it yields results comparable to directly tuning α on the test set. Qualitative detection results using the proposed SimEmb model can be found in Figure 5.

Alpha scaling versus uncertainty calibration. As an alternative to alpha scaling for GZSD, we evaluate the uncertainty calibration technique, as explained in Section 3.2. We present the results in Table 2, with the following combinations from top to the bottom: base model, uncertainty calibration (*uc-calib*) only, alpha scaling only, and their combination. We observe that uncertainty calibration alone performs poorly probably due to the difficulty of correcting class bias purely based on fine-tuning. Our alpha scaling technique yields a much better result in terms of HM score, with an improvement from 17.34 to 20.41. The combination of the two techniques slightly improves the HM score to 20.46. This proves that the alpha scaling scheme is effective.

Exp. Type	Test	bottle	bus	couch	microwave	pizza	racket	suitcase	zebra	U-mAP(%)	S-mAP(%)	HM
ZSD	U	5.2	53.3	35.1	23.9	44.4	36.4	9.1	43.7	31.4	-	-
GZSD w/o α	S+U	0	0	2.7	0	0	0	0	0	0.3	27.4	0.7
GZSD	S+U	0.8	21.4	4.9	1.2	4.8	0.7	9.1	15.8	7.3	19.2	10.6

TABLE 3: Our results on ZSD and GZSD (72/8). In this table, the first row represents the experimental results where we only use images belong to the unseen classes and unseen class vectors, remaining rows represent the generalized zero-shot object detection results where we use seen and unseen class vectors together on MS-COCO val5k split.

Method	bottle	bus	couch	microwave	pizza	racket	suitcase	zebra	Avg. F1	METEOR	SPICE
True zero-shot captioning											
NBT-baseline	0	0	0	0	0	0	0	0	0	18.2	12.7
Our method	2.4	75.2	26.6	24.6	29.8	3.6	0.6	75.4	29.8	21.9	14.2
Partial zero-shot captioning (upper-bounds)											
DCC [13]	4.6	29.8	45.9	28.1	64.6	52.2	13.2	79.9	39.8	21.0	14.4
NOC [78]	17.8	68.8	25.6	24.7	69.3	68.1	39.9	89.0	49.1	21.4	-
C-LSTM [28]	29.7	74.4	38.8	27.8	68.2	70.3	44.8	91.4	55.7	23.0	-
Base+T4 [79]	16.3	67.8	48.2	29.7	77.2	57.1	49.9	85.7	54.0	23.3	15.9
NBT+G [15]	14.0	74.8	42.8	63.7	74.4	19.0	44.5	92.0	53.2	23.9	16.6
DNOC [80]	33.0	77.0	54.0	46.6	75.8	33.0	59.5	84.6	57.9	21.6	-

TABLE 4: Zero-shot captioning results with comparison to captioning models involving visually fully-supervised models.

tive in comparison to a state-of-the-art generalized zero-shot learning calibration technique. Since the improvement from the both techniques is only marginal, for the sake of simplify, we keep using only alpha scaling in our following experiments.

GZSD results on ZSC splits. In our experiments presented so far, we have used the 65/15 COCO split, to be compatible with the GZSD literature. In our ZSC experiments, however, we need to use the alternative 72/8 split of [13] to make comparisons to the related work. Therefore, here we report the results of our GZSD model on the 72/8 split. We train the model using the same hyper-parameters as before. We select 8 out of 72 seen classes as unseen-imitation classes for alpha scaling optimization.

We evaluate the detection model on the 72/8 split under the ZSD and GZSD scenarios. For the ZSD experiments, we use the MS-COCO validation images consisting of unseen class instances. For the GZSD experiments, we use the whole MS-COCO val5k split. We present the results on Table 3. In the case of ZSD scenario, we observe an unseen class mAP of 31.4%. In the case of GZSD scenario, we observe a much lower 0.3% mAP without alpha scaling, and 0.7 HM. Alpha scaling improves the unseen class mAP to 7.3% and the HM score to 10.6. We note that prior works on GZSD do not use this ZSC (72/8) split, therefore, we do not report any comparisons to the state-of-the-art in this split. We also note that our primary interest in GZSD is to build a strong method to serve as a crucial component of zero-shot captioning, therefore, these results highlight one of the major difficulties in building accurate captioning models in the realistic ZSC setting.

5.3 Zero-Shot image captioning

For the zero-shot captioning experiments, we use the same experimental setup described in [15], and exclude the

image-sentence pairs containing unseen class instances during training. We consider the partial zero-shot captioning approaches proposed in [13], [15], [28], [78], [79] as upper-bound baselines for our true zero-shot captioning setting. We also define and evaluate a baseline method based on NBT, where we train the NBT captioning model based solely on the training classes without integrating our GZSD model. We refer to this model as *NBT-baseline*.

To establish a fair comparison, we follow the practices of the NBT [15] approach. We evaluate the ZSC model on the selected validation subset of the MS-COCO caption dataset. To obtain per-class evaluation scores, we use the F1 metric [13], where a visual class is considered as relevant in an image if that class name appears in any one of the human generated reference captions for that image, and irrelevant otherwise. Similarly, on a test image, a model-generated caption is considered as correct for a visual class if the generated caption includes (excludes) the corresponding word for that relevant (irrelevant) class. The per-class F1 score is then defined as the ratio of correctly captioned test images. We additionally use the well-established METEOR [81] and SPICE [82] metrics, in addition to averaging the per-class F1 scores (referred to as *Avg. F1*). We separately discuss the evaluation results in terms of the proposed V-METEOR metric in the next section.

We present the results in Table 4. First, we observe that the proposed approach greatly outperforms the NBT-baseline with clear improvements in terms of Avg. F1 (0 to 29.8), METEOR (18.2 to 21.9) and SPICE (12.7 to 14.2) scores. This shows the value of explicitly handling the GZSD task as part of the captioning process. In comparison to the upper-bound partial-ZSC captioning approaches, which involve supervised visual training in both seen and unseen classes, our approach yields comparable results in terms of METEOR and SPICE metrics. In particular, we observe that the ZSC model yields better results compared to the

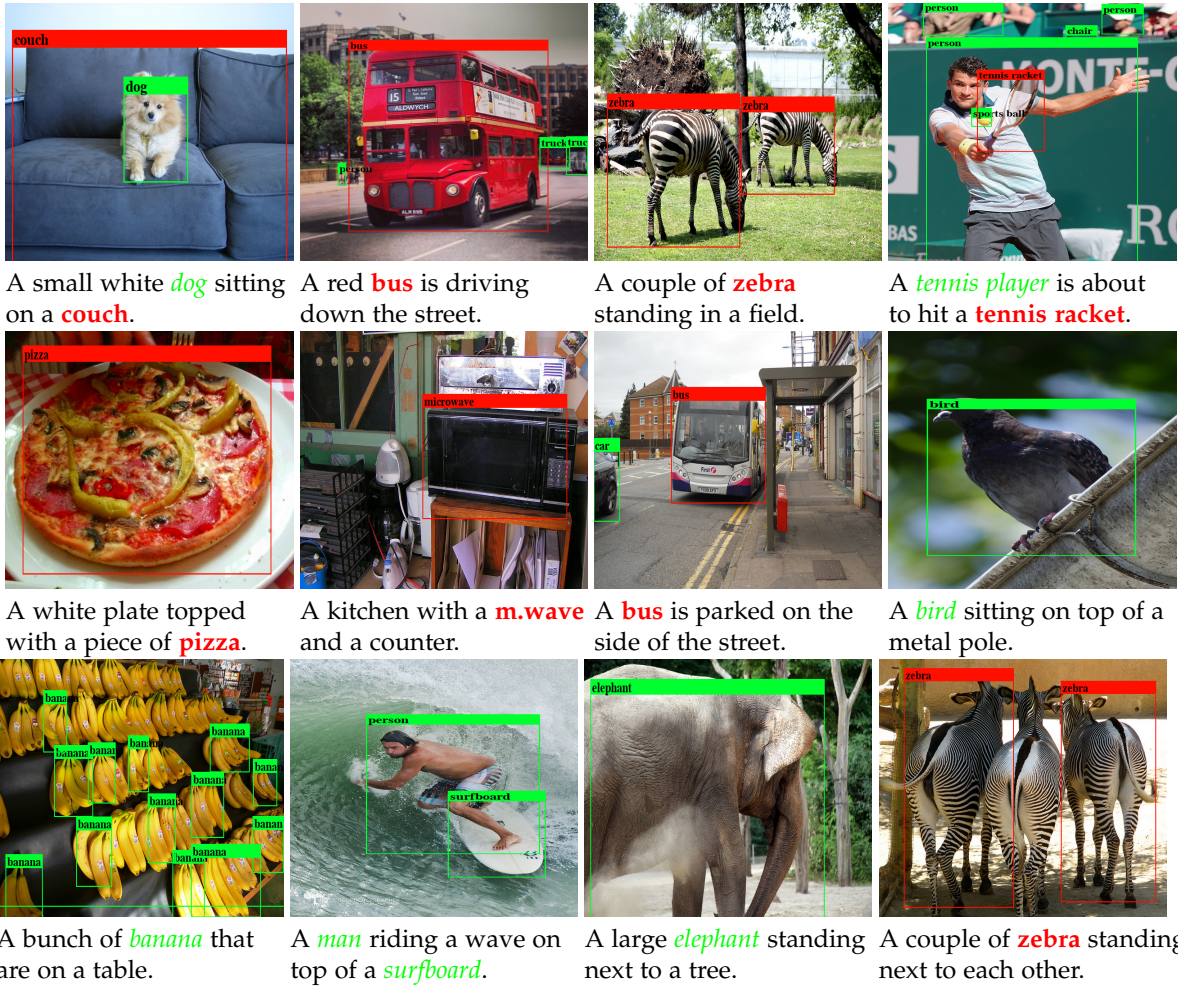


Fig. 7: Image captioning results on images with *seen* and *unseen* class instances. (Best viewed in color.)

DCC [13] and NOC [78] methods. This is most probably due to the fact that the our sentence template generation method provides accurate locations for visual words, enabling the generation of more natural and visually grounded captions. We observe relatively lower scores for the ZSC model, compared to the remaining supervised models.

Noticeably, the performance gap between true zero-shot and (visually) supervised partial zero-shot captioning is larger in terms of the Avg. F1 metric. This is mostly an expected result as the F1 metric directly measures the ability to incorporate visual classes during captioning, akin to a visual recognition metric. Here, supervised methods are known to perform much better than the state-of-the-art zero-shot learning models in most cases, which turns out to also be the case in captioning.

For qualitative examination, we present visual output examples in Figure 7, along with the corresponding GZSD detection results. It can be observed that the ZSC model is able to generate semantically sound captions in a variety of challenging scenes involving both seen and unseen class instances.

5.4 V-METEOR experiments

In this section, we evaluate the baseline and proposed models using the V-METEOR metric. We present the overall av-

Method	V-METEOR _{vis}	V-METEOR _{nvis}	V-METEOR
NBT-Baseline	0.0	20.50	0.0
Our Method	12.63	22.26	13.19

TABLE 5: V-METEOR comparison results. V-METEOR_{vis} represents a sub-metric that only includes results for visual words, and V-METEOR_{nvis} represents another sub-metric that only includes non-visual words.

erage V-METEOR scores in Table 5. These summary results show that the proposed approach greatly improves visual captioning score from 0.0 to 12.63 and also increases the non-visual V-METEOR scores from 20.50 to 22.26. The final V-METEOR score improves from 0.0 to 13.19. These results show that the integration of an (accurate) GZSD can not only help with visual coverage of the captioning results but also improve the non-visual parts of the generated captions thanks to the better visual information from the detector to the language model. In these results, we also observe the main advantage of the proposed V-METEOR metric by being able to separately discuss visual and non-visual quality of the generated captions.

To better understand the captioning results, we present per-class V-METEOR scores for the unseen classes in Fig-

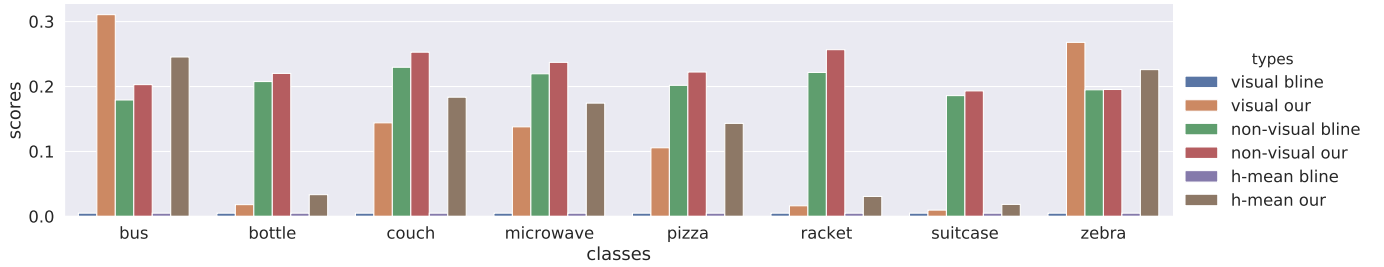


Fig. 8: V-METEOR results of each unseen classes. Here, there are six different results of NBT-Baseline and our method: **visual-bs** represents the visual meteor scores of the NBT-Baseline, **non-visual-bs** represents the non-visual meteor scores of the NBT-Baseline and **hm-bs** represents the V-METEOR scores of the NBT-Baseline method. Similarly, **visual**, **non-visual** and **hm** bars represents results of our method. (Best viewed in color.)

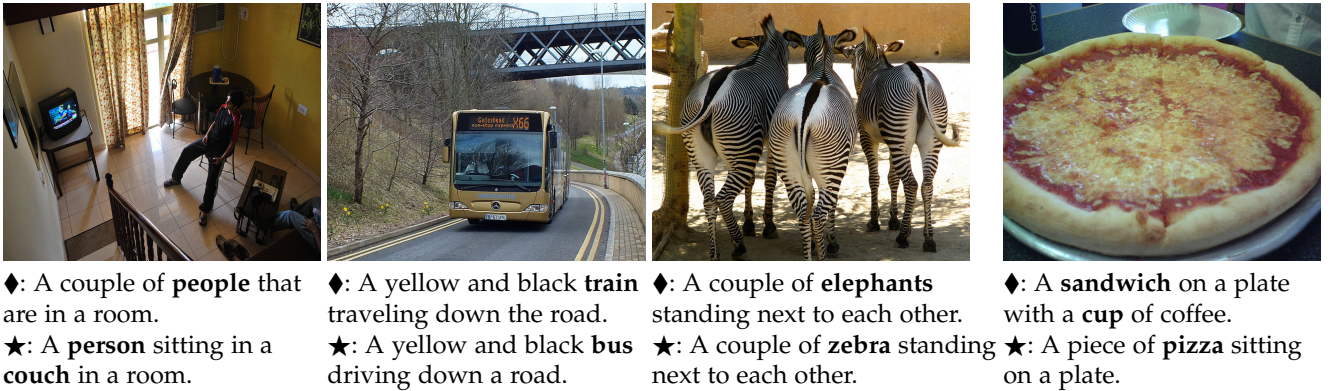


Fig. 9: Image captioning results of NBT-baseline and our methods. ♦ represents the NBT-baseline results, and ★ represents the results of the proposed method. **Bold** type words represent visual words from detectors.

ure 8. In these results, we again observe both the most significant improvements are in $V\text{-METEOR}_{\text{vis}}$ scores with still noticeable improvements in non-visual scores. The complementary qualitative captioning comparisons presented in Figure 9 supports these quantitative observations: in the *person* and *bus* examples, the whole sentence changes and improves with the correction in visual details. In the *bus* and *zebra* examples, we observe that the NBT-baseline method produces coarsely plausible sentences, however, with incorrect visual coverage due to confusions across visually similar classes. The last example shows a case where the baseline method captions a contextually coherent pair of *sandwich* (incorrect) and *cup* (correct), the proposed model corrects the *sandwich* to *pizza* but misses the *cup* in the scene.

5.5 Additional analyses

In this section, we present a quantitative analysis on the error patterns and an ablative study on the importance of proposed similarity embeddings in GZSD.

5.5.1 Diagnosing errors

The experimental results show that GZSD plays a central role in achieving accurate captioning results. Therefore, it is potentially valuable to understand the typical detection errors of our GZSD model, towards building better GZSD and ZSC approaches. For this purpose, we embrace the detector analysis approach by Hoiem *et al.* [88], which

is originally proposed for analyzing false positives in supervised detectors. The original analysis approach defines semantic categories for the PASCAL VOC dataset. To utilize this technique in the GZSD setting, we use the MSCOCO super-classes, namely *vehicle*, *outdoor*, *animal*, *accessory*, *sports*, *kitchen*, *food*, *furniture*, *electronic*, *appliance* and *indoor*, as defined in [31]. Following [88], we additionally define a separate singleton super-class for the *person* class, as it contains a greatly larger number of instances and its overall distinct visual characteristics.

The following four misdetection categories are examined for each super-class: (i) localization errors, corresponding to detections considered as false positive due to poor localization, (ii) confusion with background, counting false positive detections located in the background, (iii) class confusion within super-class members, and (iv) class confusion across super-classes. The corresponding error distributions are shown in Figure 10.

The obtained error distribution results show that the false positives are mainly occurred due to the within super-class confusions for the *vehicle*, *animal*, *accessory*, *sports*, *kitchen* and *food* super-classes. The dominant misdetection type for the *furniture*, *appliance* and *indoor* super-classes is confusion with other classes. In contrast, most *person* misdetections correspond to localization errors. Finally, we observe that most problematic detections for *outdoor* and *electronic* super-classes correspond to background detections. Overall, these results show that there is no single

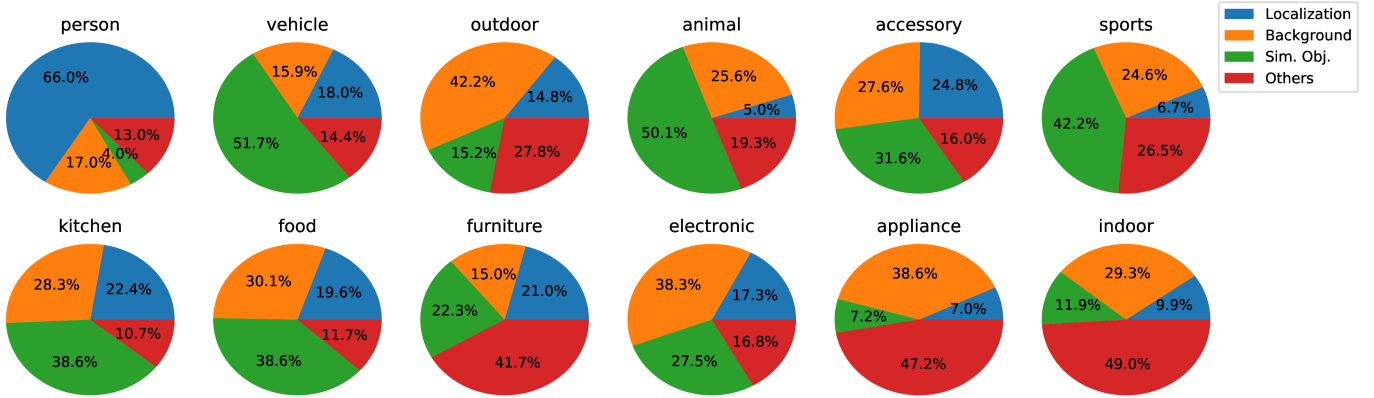


Fig. 10: False positive analyses for super-classes on MS-COCO. **Localization** represents detections considered as false positive due to poor localization, **Background** represents false positive detections located in the background, **Sim. Obj.** stands for misclassifications within super-class members and **Others** stands for confusion with other classes. (Best viewed in color.)

Method	seen/unseen	seen	unseen	HM
VW	65/15	28.41	14.36	19.08
SimEmb	65/15	28.91	15.78	20.41

TABLE 6: mAP results on MS-COCO dataset with GZSD (65/15) settings. Here, **VW** represents using class name word embeddings directly and **SimEmb** represents the class-to-class similarity based class embeddings.

error pattern dominating the GZSD outputs, and errors vary greatly across the classes.

5.5.2 Impact of using similarity embeddings

One of the advantages of using the proposed class-to-class similarity vectors is that each dimension of the embedding explicitly correspond to a class relevance value. We additionally utilize its structure in the design of our alpha scaling training scheme. To better understand the value of the proposed class embeddings for GZSD, we present a direct comparison between using the proposed class embeddings versus the original class name word embeddings.

We present the results based on both embeddings in Table 6. In the table, VW corresponds to using the word vectors directly. The results show that the more traditional VW embedding scheme obtains 28.41% mAP on seen classes, 14.36% mAP on unseen classes and a harmonic mean score of 19.08. In contrast, the proposed embedding yields 28.91% mAP on seen classes, 15.78% mAP on unseen classes and 20.41 harmonic mean score. These results show that using class-to-class similarity vectors also provides a relative performance advantage in terms of model performance, with additional benefits of simplifying the alpha coefficient optimization.

6 CONCLUSION

An important shortcoming of current image captioning methods that aim training through non-paired datasets is that they do not work in a fully zero-shot learning setting. These methods generate captions for images which consist

of classes not seen in captioning datasets, but they assume that there is a ready-to-use fully supervised visual recognition model. To this end, we define the zero-shot image captioning problem, and propose a novel generalized zero-shot object detection model and a zero-shot captioning approach based on it. We additionally introduce a practical class embedding scheme, a technique to improve generalized zero-shot detection performance via score scaling, and a novel evaluation method that provides insights to the zero-shot captioning results. Our qualitative and quantitative experimental results on show that our method yields promising results towards achieving our zero-shot captioning goals. We believe that zero-shot captioning is an important research direction towards building captioning models that are more suitable to use in realistic, in-the-wild settings.

REFERENCES

- [1] J. Redmon and A. Farhadi, “Yolo9000: Better, faster, stronger,” in *Proc. IEEE Conf. Comput. Vis. Pattern Recog.*, 2017, pp. 7263–7271.
- [2] J. Redmon, S. Divvala, R. Girshick, and A. Farhadi, “You only look once: Unified, real-time object detection,” in *Proc. IEEE Conf. Comput. Vis. Pattern Recog.*, 2016, pp. 779–788.
- [3] R. Girshick, “Fast r-cnn,” in *Proc. IEEE Int. Conf. on Computer Vision*, 2015, pp. 1440–1448.
- [4] P. Sermanet, D. Eigen, X. Zhang, M. Mathieu, R. Fergus, and Y. LeCun, “Overfeat: Integrated recognition, localization and detection using convolutional networks,” in *Proc. Int. Conf. Learn. Represent.*, 2014.
- [5] S. Bell, C. Lawrence Zitnick, K. Bala, and R. Girshick, “Inside-outside net: Detecting objects in context with skip pooling and recurrent neural networks,” in *Proc. IEEE Conf. Comput. Vis. Pattern Recog.*, 2016, pp. 2874–2883.
- [6] S. Ren, K. He, R. Girshick, and J. Sun, “Faster r-cnn: Towards real-time object detection with region proposal networks,” in *Proc. Adv. Neural Inf. Process. Syst.*, 2015, pp. 91–99.
- [7] T.-Y. Lin, P. Dollár, R. Girshick, K. He, B. Hariharan, and S. Belongie, “Feature pyramid networks for object detection,” in *Proc. IEEE Conf. Comput. Vis. Pattern Recog.*, 2017.
- [8] W. Liu, D. Anguelov, D. Erhan, C. Szegedy, S. Reed, C.-Y. Fu, and A. C. Berg, “Ssd: Single shot multibox detector,” in *Proc. European Conf. on Computer Vision*. Springer, 2016, pp. 21–37.
- [9] J. Yan, Z. Lei, L. Wen, and S. Li, “The fastest deformable part model for object detection,” in *Proc. IEEE Conf. Comput. Vis. Pattern Recog.*, 2014, pp. 2497–2504.

- [10] T.-Y. Lin, P. Goyal, R. Girshick, K. He, and P. Dollár, "Focal loss for dense object detection," *IEEE Trans. Pattern Anal. Mach. Intell.*, 2018.
- [11] H. Law and J. Deng, "Cornernet: Detecting objects as paired keypoints," in *Proc. European Conf. on Computer Vision*, 2018, pp. 734–750.
- [12] G. Kulkarni, V. Premraj, V. Ordonez, S. Dhar, S. Li, Y. Choi, A. C. Berg, and T. L. Berg, "Babytalk: Understanding and generating simple image descriptions," *IEEE Trans. Pattern Anal. Mach. Intell.*, vol. 35, no. 12, pp. 2891–2903, 2013.
- [13] L. Anne Hendricks, S. Venugopalan, M. Rohrbach, R. Mooney, K. Saenko, and T. Darrell, "Deep compositional captioning: Describing novel object categories without paired training data," in *Proc. IEEE Conf. Comput. Vis. Pattern Recog.*, 2016, pp. 1–10.
- [14] X. Yin and V. Ordonez, "Obj2text: Generating visually descriptive language from object layouts," in *Proc. of the Empirical Methods in Natural Language Processing*, 2017, pp. 177–187.
- [15] J. Lu, J. Yang, D. Batra, and D. Parikh, "Neural baby talk," in *Proc. IEEE Conf. Comput. Vis. Pattern Recog.*, 2018, pp. 7219–7228.
- [16] Z. Akata, F. Perronnin, Z. Harchaoui, and C. Schmid, "Label-embedding for attribute-based classification," in *Proc. IEEE Conf. Comput. Vis. Pattern Recog.* IEEE, 2013, pp. 819–826.
- [17] D. Jayaraman and K. Grauman, "Zero-shot recognition with unreliable attributes," in *Proc. Adv. Neural Inf. Process. Syst.*, 2014, pp. 3464–3472.
- [18] M. Rohrbach, M. Stark, and B. Schiele, "Evaluating knowledge transfer and zero-shot learning in a large-scale setting," in *Proc. IEEE Conf. Comput. Vis. Pattern Recog.* IEEE, 2011, pp. 1641–1648.
- [19] Z. Akata, S. Reed, D. Walter, H. Lee, and B. Schiele, "Evaluation of output embeddings for fine-grained image classification," in *Proc. IEEE Conf. Comput. Vis. Pattern Recog.* IEEE Computer Society, 2015.
- [20] B. Demirel, R. G. Cinbis, and N. Ikizler-Cinbis, "Attributes2classname: A discriminative model for attribute-based unsupervised zero-shot learning," in *Proc. IEEE Int. Conf. on Computer Vision*, Oct 2017.
- [21] J. Deng, N. Ding, Y. Jia, A. Frome, K. Murphy, S. Bengio, Y. Li, H. Neven, and H. Adam, "Large-scale object classification using label relation graphs," in *Proc. European Conf. on Computer Vision*, 2014, pp. 48–64.
- [22] Y. Xian, C. H. Lampert, B. Schiele, and Z. Akata, "Zero-shot learning—a comprehensive evaluation of the good, the bad and the ugly," *IEEE Trans. Pattern Anal. Mach. Intell.*, vol. 41, no. 9, pp. 2251–2265, 2018.
- [23] B. Demirel, R. G. Cinbis, and N. Ikizler-Cinbis, "Zero-shot object detection by hybrid region embedding," in *British Machine Vision Conf.*, 2018, p. 56.
- [24] S. Rahman, S. Khan, and F. Porikli, "Zero-shot object detection: Learning to simultaneously recognize and localize novel concepts," in *Asian Conf. on Computer Vision*. Springer, 2018, pp. 547–563.
- [25] A. Bansal, K. Sikka, G. Sharma, R. Chellappa, and A. Divakaran, "Zero-shot object detection," in *Proc. European Conf. on Computer Vision*, 2018, pp. 384–400.
- [26] S. Rahman, S. Khan, and N. Barnes, "Polarity loss for zero-shot object detection," *arXiv preprint arXiv:1811.08982*, 2018.
- [27] S. Rahman, S. Khan, and N. Barnes, "Transductive learning for zero-shot object detection," in *Proc. IEEE Conf. Comput. Vis. Pattern Recog.*, 2019, pp. 6082–6091.
- [28] T. Yao, Y. Pan, Y. Li, and T. Mei, "Incorporating copying mechanism in image captioning for learning novel objects," in *Proc. IEEE Conf. Comput. Vis. Pattern Recog.*, 2017, pp. 6580–6588.
- [29] S. Liu, M. Long, J. Wang, and M. I. Jordan, "Generalized zero-shot learning with deep calibration network," in *Proc. Adv. Neural Inf. Process. Syst.*, 2018, pp. 2005–2015.
- [30] T. Mikolov, I. Sutskever, K. Chen, G. S. Corrado, and J. Dean, "Distributed representations of words and phrases and their compositionality," in *Proc. Adv. Neural Inf. Process. Syst.*, 2013, pp. 3111–3119.
- [31] T.-Y. Lin, M. Maire, S. Belongie, J. Hays, P. Perona, D. Ramanan, P. Dollár, and C. L. Zitnick, "Microsoft coco: Common objects in context," in *Proc. European Conf. on Computer Vision*, 2014, pp. 740–755.
- [32] B. Demirel, R. G. Cinbis, and N. Ikizler-Cinbis, "Image captioning with unseen objects," in *British Machine Vision Conf.*, 2019, p. 146.
- [33] C. H. Lampert, H. Nickisch, and S. Harmeling, "Learning to detect unseen object classes by between-class attribute transfer," in *Proc. IEEE Conf. Comput. Vis. Pattern Recog.*, 2009, pp. 951–958.
- [34] S. Changpinyo, W.-L. Chao, B. Gong, and F. Sha, "Synthesized classifiers for zero-shot learning," in *Proc. IEEE Conf. Comput. Vis. Pattern Recog.*, 2016, pp. 5327–5336.
- [35] E. Kodirov, T. Xiang, and S. Gong, "Semantic autoencoder for zero-shot learning," in *Proc. IEEE Conf. Comput. Vis. Pattern Recog.*, 2017, pp. 3174–3183.
- [36] Y. Long, L. Liu, F. Shen, L. Shao, and X. Li, "Zero-shot learning using synthesised unseen visual data with diffusion regularisation," *IEEE Trans. Pattern Anal. Mach. Intell.*, vol. 40, no. 10, pp. 2498–2512, 2018.
- [37] C. Luo, Z. Li, K. Huang, J. Feng, and M. Wang, "Zero-shot learning via attribute regression and class prototype rectification," *IEEE Trans. on Image Processing*, vol. 27, no. 2, pp. 637–648, 2018.
- [38] Y. Yu, Z. Ji, J. Guo, and Z. Zhang, "Zero-shot learning via latent space encoding," *IEEE transactions on cybernetics*, no. 99, pp. 1–12, 2018.
- [39] S. Liu, M. Long, J. Wang, and M. I. Jordan, "Generalized Zero-Shot Learning with Deep Calibration Network," in *Proc. Adv. Neural Inf. Process. Syst.*, 2018.
- [40] H. Jiang, R. Wang, S. Shan, and X. Chen, "Transferable Contrastive Network for Generalized Zero-Shot Learning," in *Proc. IEEE Int. Conf. on Computer Vision*, Aug. 2019.
- [41] J. Song, C. Shen, Y. Yang, Y. Liu, and M. Song, "Transductive unbiased embedding for zero-shot learning," in *Proc. IEEE Conf. Comput. Vis. Pattern Recog.*, 2018, pp. 1024–1033.
- [42] W.-L. Chao, S. Changpinyo, B. Gong, and F. Sha, "An empirical study and analysis of generalized zero-shot learning for object recognition in the wild," in *Proc. European Conf. on Computer Vision*. Springer, 2016, pp. 52–68.
- [43] M. Bucher, S. Herbin, and F. Jurie, "Generating visual representations for zero-shot classification," in *Proc. IEEE Int. Conf. on Computer Vision Workshops*, 2017, pp. 2666–2673.
- [44] R. Felix, V. B. Kumar, I. Reid, and G. Carneiro, "Multi-modal cycle-consistent generalized zero-shot learning," in *Proc. European Conf. on Computer Vision*, 2018, pp. 21–37.
- [45] A. Mishra, S. Krishna Reddy, A. Mittal, and H. A. Murthy, "A generative model for zero shot learning using conditional variational autoencoders," in *Proc. IEEE Conf. Comput. Vis. Pattern Recog. Workshops*, 2018, pp. 2188–2196.
- [46] D. P. Kingma and M. Welling, "Auto-encoding variational bayes," in *Proc. Int. Conf. Learn. Represent.*, 2014.
- [47] D. J. Rezende, S. Mohamed, and D. Wierstra, "Stochastic back-propagation and approximate inference in deep generative models," in *Proc. Int. Conf. Mach. Learn.* PMLR, 2014, pp. 1278–1286.
- [48] Y. Xian, S. Sharma, B. Schiele, and Z. Akata, "f-vaegan-d2: A feature generating framework for any-shot learning," in *Proc. IEEE Conf. Comput. Vis. Pattern Recog.*, 2019, pp. 10 275–10 284.
- [49] Y. Zhu, M. Elhoseiny, B. Liu, X. Peng, and A. Elgammal, "A generative adversarial approach for zero-shot learning from noisy texts," in *Proc. IEEE Conf. Comput. Vis. Pattern Recog.*, 2018, pp. 1004–1013.
- [50] J. Li, M. Jing, K. Lu, Z. Ding, L. Zhu, and Z. Huang, "Leveraging the invariant side of generative zero-shot learning," in *Proc. IEEE Conf. Comput. Vis. Pattern Recog.*, 2019, pp. 7402–7411.
- [51] M. B. Sariyildiz and R. G. Cinbis, "Gradient matching generative networks for zero-shot learning," in *Proc. IEEE Conf. Comput. Vis. Pattern Recog.*, 2019, pp. 2168–2178.
- [52] M. Elhoseiny and M. Elfeki, "Creativity inspired zero-shot learning," in *Proc. IEEE Conf. Comput. Vis. Pattern Recog.*, 2019, pp. 5784–5793.
- [53] Z. Shen, Z. Liu, J. Li, Y.-G. Jiang, Y. Chen, and X. Xue, "Dsod: Learning deeply supervised object detectors from scratch," in *Proc. IEEE Int. Conf. on Computer Vision*, 2017, pp. 1919–1927.
- [54] C.-Y. Fu, W. Liu, A. Ranga, A. Tyagi, and A. C. Berg, "Dssd: Deconvolutional single shot detector," *arXiv preprint arXiv:1701.06659*, 2017.
- [55] K. He, X. Zhang, S. Ren, and J. Sun, "Spatial pyramid pooling in deep convolutional networks for visual recognition," *IEEE Trans. Pattern Anal. Mach. Intell.*, vol. 37, no. 9, pp. 1904–1916, 2015.
- [56] J. Dai, Y. Li, K. He, and J. Sun, "R-fcn: Object detection via region-based fully convolutional networks," in *Proc. Adv. Neural Inf. Process. Syst.*, 2016, pp. 379–387.

- [57] Z. Li, L. Yao, X. Zhang, X. Wang, S. Kanhere, and H. Zhang, "Zero-shot object detection with textual descriptions," in *Proc. of the AAAI Conf. on Artificial Intelligence*, vol. 33, 2019, pp. 8690–8697.
- [58] Y. Shao, Y. Li, and D. Wang, "Zero-shot detection with transferable object proposal mechanism," in *IEEE Int. Conf. on Image Processing*. IEEE, 2019, pp. 3666–3670.
- [59] C. L. Zitnick and P. Dollár, "Edge boxes: Locating object proposals from edges," in *Proc. European Conf. on Computer Vision*, 2014, pp. 391–405.
- [60] M. Norouzi, T. Mikolov, S. Bengio, Y. Singer, J. Shlens, A. Frome, G. S. Corrado, and J. Dean, "Zero-shot learning by convex combination of semantic embeddings," in *Proc. Int. Conf. Learn. Represent.*, 2014.
- [61] J. Hoffman, S. Guadarrama, E. S. Tzeng, R. Hu, J. Donahue, R. Girshick, T. Darrell, and K. Saenko, "Lsda: Large scale detection through adaptation," in *Proc. Adv. Neural Inf. Process. Syst.*, 2014, pp. 3536–3544.
- [62] J. Hoffman, D. Pathak, T. Darrell, and K. Saenko, "Detector discovery in the wild: Joint multiple instance and representation learning," in *Proc. IEEE Conf. Comput. Vis. Pattern Recog.*, 2015, pp. 2883–2891.
- [63] R. G. Cinbis, J. Verbeek, and C. Schmid, "Weakly supervised object localization with multi-fold multiple instance learning," *IEEE Trans. Pattern Anal. Mach. Intell.*, vol. 39, no. 1, pp. 189–203, 2016.
- [64] A. Arun, C. Jawahar, and M. P. Kumar, "Dissimilarity Coefficient Based Weakly Supervised Object Detection," in *Proc. IEEE Conf. Comput. Vis. Pattern Recog.*, Long Beach, CA, USA, Jun. 2019, pp. 9424–9433.
- [65] Z. Ren, Z. Yu, X. Yang, M.-Y. Liu, Y. J. Lee, A. G. Schwing, and J. Kautz, "Instance-aware, context-focused, and memory-efficient weakly supervised object detection," in *Proc. IEEE Conf. Comput. Vis. Pattern Recog.*, 2020, pp. 10 598–10 607.
- [66] J. Mao, W. Xu, Y. Yang, J. Wang, Z. Huang, and A. Yuille, "Deep captioning with multimodal recurrent neural networks (m-rnn)," *Proc. Int. Conf. Learn. Represent.*, 2015.
- [67] Q. You, H. Jin, Z. Wang, C. Fang, and J. Luo, "Image captioning with semantic attention," in *Proc. IEEE Conf. Comput. Vis. Pattern Recog.*, 2016, pp. 4651–4659.
- [68] K. Xu, J. Ba, R. Kiros, K. Cho, A. Courville, R. Salakhudinov, R. Zemel, and Y. Bengio, "Show, attend and tell: Neural image caption generation with visual attention," in *Proc. Int. Conf. Mach. Learn.*, 2015, pp. 2048–2057.
- [69] R. Kiros, R. Salakhudinov, and R. S. Zemel, "Unifying visual-semantic embeddings with multimodal neural language models," *arXiv preprint arXiv:1411.2539*, 2014.
- [70] A. Karpathy and L. Fei-Fei, "Deep visual-semantic alignments for generating image descriptions," in *Proc. IEEE Conf. Comput. Vis. Pattern Recog.*, 2015, pp. 3128–3137.
- [71] A. Farhadi, M. Hejrati, M. A. Sadeghi, P. Young, C. Rashtchian, J. Hockenmaier, and D. Forsyth, "Every picture tells a story: Generating sentences from images," in *Proc. European Conf. on Computer Vision*. Springer, 2010, pp. 15–29.
- [72] M. Hodosh, P. Young, and J. Hockenmaier, "Framing image description as a ranking task: Data, models and evaluation metrics," *Journal of Artificial Intelligence Research*, vol. 47, pp. 853–899, 2013.
- [73] V. Ordonez, G. Kulkarni, and T. L. Berg, "Im2text: Describing images using 1 million captioned photographs," in *Proc. Adv. Neural Inf. Process. Syst.*, 2011, pp. 1143–1151.
- [74] C. Sun, C. Gan, and R. Nevatia, "Automatic concept discovery from parallel text and visual corpora," in *Proc. IEEE Int. Conf. on Computer Vision*, 2015, pp. 2596–2604.
- [75] J. Johnson, A. Karpathy, and L. Fei-Fei, "Densecap: Fully convolutional localization networks for dense captioning," in *Proc. IEEE Conf. Comput. Vis. Pattern Recog.*, 2016, pp. 4565–4574.
- [76] L. Yang, K. Tang, J. Yang, and L.-J. Li, "Dense captioning with joint inference and visual context," in *Proc. IEEE Conf. Comput. Vis. Pattern Recog.*, 2017, pp. 2193–2202.
- [77] R. Krishna, K. Hata, F. Ren, L. Fei-Fei, and J. Carlos Niebles, "Dense-captioning events in videos," in *Proc. IEEE Conf. Comput. Vis. Pattern Recog.*, 2017, pp. 706–715.
- [78] S. Venugopalan, L. Anne Hendricks, M. Rohrbach, R. Mooney, T. Darrell, and K. Saenko, "Captioning images with diverse objects," in *Proc. IEEE Conf. Comput. Vis. Pattern Recog.*, 2017, pp. 5753–5761.
- [79] P. Anderson, B. Fernando, M. Johnson, and S. Gould, "Guided open vocabulary image captioning with constrained beam search," in *Proc. of the Empirical Methods in Natural Language Processing*, 2017, pp. 936–945.
- [80] Y. Wu, L. Zhu, L. Jiang, and Y. Yang, "Decoupled novel object captioner," in *Proc. of the 26th ACM international conf. on Multimedia*, 2018, pp. 1029–1037.
- [81] M. Denkowski and A. Lavie, "Meteor universal: Language specific translation evaluation for any target language," in *Proc. of the ninth workshop on statistical machine translation*, 2014, pp. 376–380.
- [82] P. Anderson, B. Fernando, M. Johnson, and S. Gould, "Spice: Semantic propositional image caption evaluation," in *Proc. European Conf. on Computer Vision*. Springer, 2016, pp. 382–398.
- [83] Z. Wang, B. Feng, K. Narasimhan, and O. Russakovsky, "Towards unique and informative captioning of images," in *Proc. European Conf. on Computer Vision*, 2020, pp. 629–644.
- [84] J. Pennington, R. Socher, and C. Manning, "Glove: Global vectors for word representation," in *Proc. of the Empirical Methods in Natural Language Processing*, 2014, pp. 1532–1543.
- [85] O. Vinyals, M. Fortunato, and N. Jaitly, "Pointer networks," in *Proc. Adv. Neural Inf. Process. Syst.*, 2015, pp. 2692–2700.
- [86] M. Kilickaya, A. Erdem, N. Ikizler-Cinbis, and E. Erdem, "Re-evaluating automatic metrics for image captioning," in *Proc. of the 15th Conference of the European Chapter of the Assoc. for Computational Linguistics*, 2017.
- [87] T. Mikolov, K. Chen, G. Corrado, and J. Dean, "Efficient estimation of word representations in vector space," *Proc. Int. Conf. Learn. Represent.*, 2013.
- [88] D. Hoiem, Y. Chodpathumwan, and Q. Dai, "Diagnosing error in object detectors," in *Proc. European Conf. on Computer Vision*, 2012, pp. 340–353.



Berkan Demirel received his BSc and MSc degrees from the Department of Computer Engineering at Hacettepe University. He is a doctoral student at METU, Ankara, Turkey and also Lead AI Engineer at HAVELSAN Inc. His research areas are machine learning and its applications in computer vision, natural language processing and remote sensing, particularly interested in learning with minimal supervision.



Ramazan Gokberk Cinbis received his Bsc degree from Bilkent University, Turkey, and received his M.A. degree from Boston University, USA. He was a doctoral student at INRIA Grenoble, France, between 2010-2014, and received a PhD degree from Université de Grenoble, France, in 2014. He is currently a faculty member at METU, Ankara, Turkey. His research interests include machine learning and computer vision, with special interest in learning with incomplete supervision.